JOURNAL OF APPLIED ELECTROCHEMISTRY 20 (1990) 418–426

The electrochemical behaviour of polycrystalline nickel electrodes in different carbonate–bicarbonate ion-containing solutions

A. E. BOHÉ, J. R. VILCHE, A. J. ARVIA

Instituto de Investigaciones Fisicoquimicas Teóricas y Aplicadas (INIFTA), Facultad de Ciencias Exactas, UNLP, Sucursal 4 – CC 16, (1900) La Plata, Argentina

Received 6 April 1989; revised 30 June 1989

The dissolution and passivation of polycrystalline nickel in carbonate–bicarbonate ion-containing solutions covering wide ranges of pH and electrolyte concentration were investigated by employing voltammetric, galvanostatic and potentiostatic transient techniques. Results obtained with a rotating disc electrode allow the competing reactions related to the active–passive transition to be distinguished through the influence of the potential sweep rate and the rotation speed on the electrochemical behaviour of the system at fixed concentrations of either carbonate or bicarbonate ion. The first oxidation level of nickel corresponds mainly to $Ni(OH)_2$ formation, the chemical dissolution of the surface layer and the precipitation of $NiCO_3$ and $Ni(OH)_2$. The partial removal of the prepassive layer is predominantly assisted by both the bicarbonate ion concentration and the electrode rotation. In the presence of chloride ions the formation of soluble Ni(II) species and $NiCo_3$ in the potential range of the first oxidation level appears to be enhanced. This effect can be interpreted by taking into account competitive adsorption processes at the base metal between Cl^- and OH^- ions.

1. Introduction

The electrochemical behaviour of the iron-group transition metals in buffered borate–boric acid solutions has been extensively studied in relation to the kinetics and mechanism of metal electrodissolution and passivation, and to the composition and structure of anodic product layers [1–11]. In general, the formation of these layers is considerably influenced by pH and the characteristics of the perturbing electrical variable, although it is practically independent of the hydrodynamic conditions. A comparable behaviour can be expected in the buffered carbonate–bicarbonate system. However, data on the dissolution and passivation of Fe [6, 12, 13], Co [4, 5, 14] and Ni [15] in solutions containing carbonate–bicarbonate ions suggest that, at constant pH, the stability of the anodic films under stirring decreases compared to that of films produced in stagnant electrolytes. The dissolution of Fe [13] and Co [14] in carbonate–bicarbonate solutions has shown that at constant pH and hydrodynamic conditions, the anodic processes associated with the active–passive transition are also influenced by the CO_3^{2-}/HCO_3^- concentration ratio. In the particular case of Ni and nickel alloys, the pitting corrosion of these metals is inhibited in alkaline solutions containing carbonate–bicarbonate [16, 17]. It is known that the passivity breakdown of nickel in 0.001–5.0 M NaOH solutions with NaCl additions occurs when a threshold Cl^-/OH^- ion concentration ratio close to 1, is exceeded [18].

This paper is devoted to the study of the active–passive transition of polycrystalline nickel in carbonate–bicarbonate solutions covering a wide range of pH and different ionic strengths, to establish the kinetics and possible mechanisms of the corresponding reactions.

2. Experimental details

The experimental setup was the same as that described in previous publications [12–14]. The working electrodes consisted of high purity polycrystalline nickel ('Specpure' from Johnson Matthey Chemicals Ltd) in the form of either fixed wire (0.5 mm diameter, 0.25 cm^2 apparent area) or rotating disc (0.070 cm^2 apparent area) axially mounted in full on a PTFE holder. Working electrodes were successively polished with 400 and 600 grade emery papers, 1.0 and 0.3 μm grit alumina–acetone suspensions and the finest grade diamond paste. Subsequently, the electrodes were thoroughly rinsed in triply distilled water. A large area Pt sheet placed in a separate cell compartment was used as counterelectrode. The latter was previously cleaned by immersion in hot concentrated hydrochloric acid and heated in the reducing zone of a gas burner. Potentials were measured against an SCE properly shielded in full, but in the text they are referred to the NHE scale in full.

Runs were made in the following solutions:

Solution A: p M K_2CO_3 ($0.02 \leqslant p \leqslant 2$) at pH 11.7 and 25° C. For these solutions the equilib-

0021-891X/90 $03.00 + .12

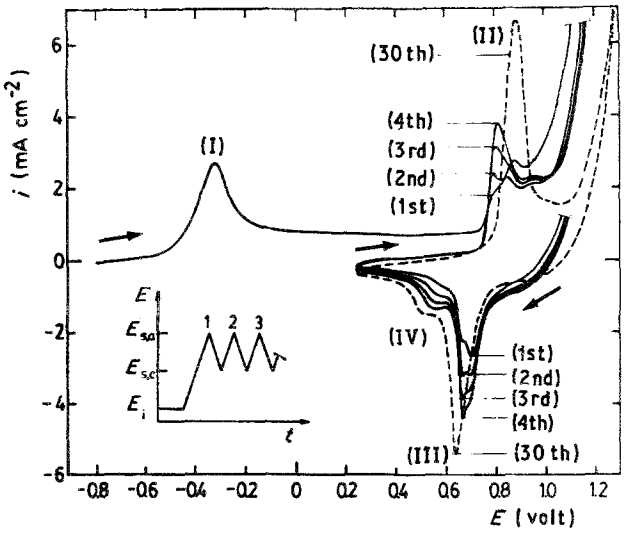

Fig. 1. Voltammogram run with still 0.5 M K_2CO_3 solution at $v = 0.25\ V\ s^{-1}$. The perturbing E/t plot is depicted in the figure. $E = -0.81$ V, $E_{s,c} = 0.24$ V and $E_{s,a} = 1.24$ V. The 1st, 2nd, 3rd, 4th and 30th potential cycles are shown.

rium CO_3^{2-}/HCO_3^- concentration ratio is close to 25.

Solution B: 0.5 M K_2CO_3 in the 0–75° C range.

Solution C: 0.5 M K_2CO_3 + q M KCl ($0 \leqslant q \leqslant 1$) at pH 11.7 and 25° C.

Solution D: x M $KHCO_3$ + y M K_2CO_3 ($0.075 \leqslant x \leqslant 2.5$, $0.0015 \leqslant y \leqslant 1.5$) covering the 8.35–11.7 pH range at 25° C. At each pH the values of x and y were set to cover a wide ionic strength range by keeping the HCO_3^-/CO_3^{2-} concentration ratio constant.

Solutions were prepared from AR (p.a. Merck) reagents and triply distrilled water previously boiled to remove CO_2.

Experiments were made under purified nitrogen gas saturation by employing one of the following perturbing programmes:

(a) single (STPS) and repetitive (RTPS) triangular potential sweeps between preset cathodic (Es, x) and anodic (Es, a) switching potentials, at potential sweep rates (v) in the $0.001\ V\ s^{-1} \leqslant v \leqslant 10\ V\ s^{-1}$ range, and working electrode rotation speed (w) in the $0 \leqslant w \leqslant 2800$ r.p.m. range;

(b) STPS and RTPS combined with different potential steps; and

(c) current steps between preset cathodic (j_c) and anodic (j_a) current densities.

The reference voltammogram (Fig. 1) obtained with a polycrystalline nickel electrode in 0.5 M K_2CO_3 at $0.25\ V\ s^{-1}$ [15] shows an anodic current peak (I) at *c.* −0.35 V, which is associated with the formation of $Ni(OH)_2$ species, and at high potentials preceding the OER multiple anodic (II) and cathodic (III–IV) peaks which are related to the $Ni(OH)_2/NiOOH$ redox system.

3. Results

3.1. *System Ni/Solution A*

The voltammograms of nickel at different v (Fig. 2) related to the active-passive transition in quiescent 0.5 M K_2CO_3 solution, pH 11.7 and 25° C, show a net anodic contribution at about −0.4 V (Peak 1). For $v < 0.25\ V\ s^{-1}$ the corresponding pseudocapacitance current and charge densities increases as v decreases (Fig. 2a), and they become practically constant for $v \geqslant 0.25\ V\ s^{-1}$. Likewise, for decreasing v, a small anodic hump at the negative potential side of peak I can be observed, probably due to the electrooxidation of hydrogen. It should be noticed, however, that the electroreduction process associated with the cathodic peak *V*, located at *c.* −0.72 V, appears to be practically independent of v after the proper HER baseline correction. Voltammograms run at different v show two isopotentials at −0.79 V and −0.53 V, respectively, which can be associated with the $Ni/Ni(OH)_2$

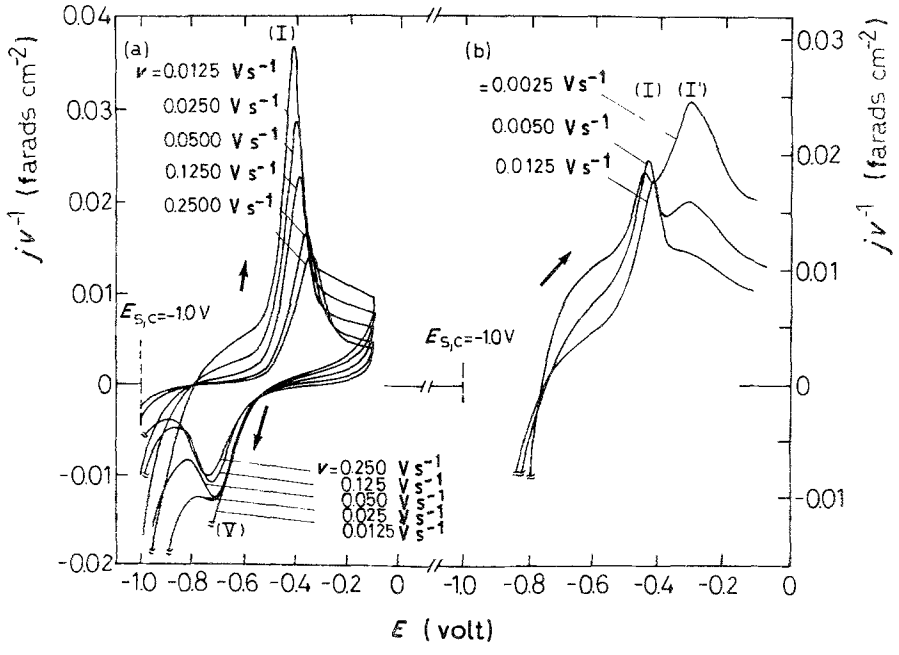

Fig. 2. Voltammograms run at different v in 0.5 M K_2CO_3 (pH = 11.7, 25° C) at (a) $w = 0$ and (b) $w = 2620$ r.p.m.

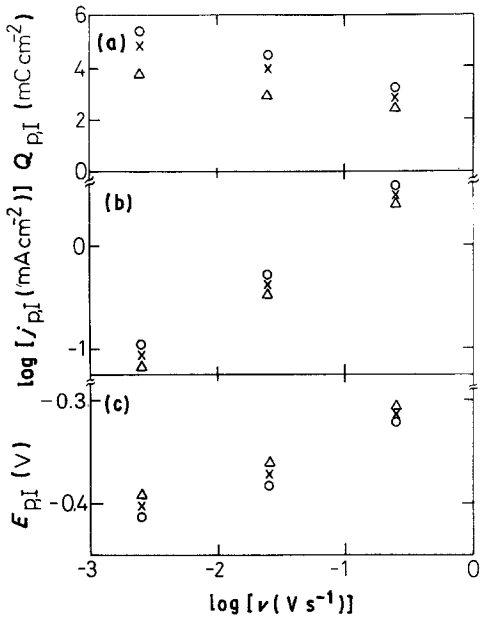

Fig. 3. Dependences of $Q_{p,I}$ (a), $j_{p,I}$ (b) and $E_{p,I}$ (c) on v from voltammograms obtained at w = 0 in, (○) 2 M K_2CO_3, (×) 0.5 M K_2CO_3 and (△) 0.02 M K_2CO_3 solutions at pH = 11.7.

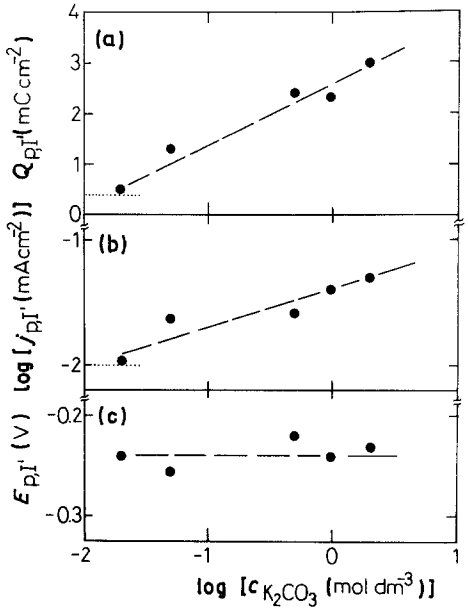

Fig. 5. Dependences of $Q_{p,I'}$ (a) $j_{p,I'}$ (b) dand $E_{p,I'}$ (c) on the K_2CO_3 concentration at pH = 11.7 from voltammograms run at v = 0.0025 V s^{-1} and w = 2620 r.p.m.

redox system [19, 20]. On the other hand, similar measurements performed with stirred solutions, i.e. for w = 2620 r.p.m. (Fig. 2b) exhibit a new anodic process (Peak I′) (at potentials more positive than that of Peak I), whose contribution increases as v decreases. Furthermore, under stirring the charge density for peak I is practically independent of v.

For Solution A at pH 11.7, Peak I in the voltammograms run with quiescent solution are little affected by the K_2CO_3 concentration, at least within the 0.02–2 M K_2CO_3 concentration range. The voltammetric charge density of Peak I ($Q_{p,I}$) increases slightly with K_2CO_3 concentration, this effect being more clearly observed as v decreases (Fig. 3a). The height of Peak I ($j_{p,I}$) fits a linear log $j_{p,I}$ against log v relationship, with a slope of about 0.80 ± 0.07 (Fig. 3b), whereas the potential of Peak I ($E_{p,I}$) changes linearly with log v, the slope of the $E_{p,I}$ against log v plot being 0.044 ± 0.007 V (decade)$^{-1}$ (Fig. 3b). Under stirring, a linear dependence of both log $j_{p,I}$ and $E_{p,I}$ on log v is also observed, the slopes of the straight lines approaching 0.98 ± 0.07 and 0.064 ± 0.007 V (decade)$^{-1}$, respectively (Fig. 4).

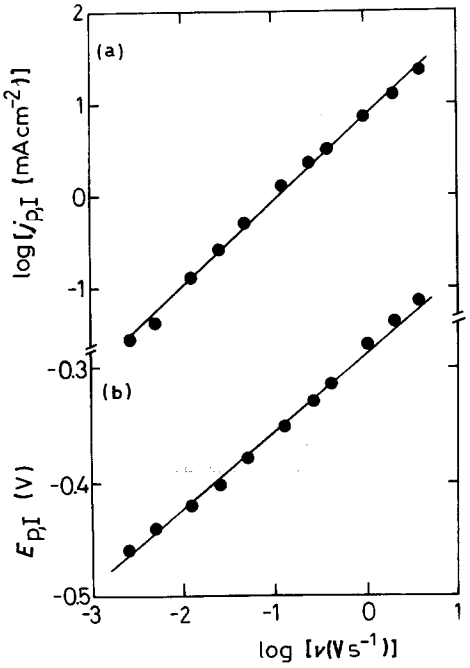

Fig. 4. Dependences of $j_{p,I}$ (a) and $E_{p,I}$ (b) on v from voltammograms run at w = 2620 r.p.m. in 0.5 M K_2CO_3.

As far as Peak IV is concerned, the voltammograms obtained at v = 0.0025 V s^{-1} and w = 2620 r.p.m. exhibit linear $Q_{p,I'}$ against log $c_{K_2CO_3}$ (Fig. 5a) and log $j_{p,I'}$ against log $c_{K_2CO_3}$ (Fig. 5b) relationships. The log $j_{p,I'}$ against log $c_{K_2CO_3}$ straight line shows a slope close to 0.4 ± 0.1. For the sake of comparison, dotted points in Figs 5a and b indicate $Q_{p,I'}$ and log $j_{p,I'}$ values, for nickel in plain KOH solution and pH 11.7 in the absence of K_2CO_3. Likewise, $E_{p,I'}$ is practically independent of the K_2CO_3 concentration (Fig. 5c). These results suggest that the kinetics of the overall electrooxidation process associated with Peak I′ in stirred solutions is remarkably influenced by the concentration of K_2CO_3 for $c_{K_2CO_3}$ > 0.02 M.

3.2. *System Ni/Solution B*

Further details of the entire passivation process in solutions containing a fixed K_2CO_3 concentration at pH 11.7 can be discovered after inspecting the influence of temperature on the characteristics of the complex peaks I/I′. The voltammetric response of nickel in quiescent 0.5 M K_2CO_3 solution in the 0–75° C range shows that the increase of $Q_{p,I}$ with decreasing v is enhanced as the temperature is increased (Fig. 6a). Under the same experimental conditions the log $j_{p,I}$ against log v plots approach a linear relationship with an average slope close to 0.8, independently of temperature, although at constant v the value of $j_{p,I}$

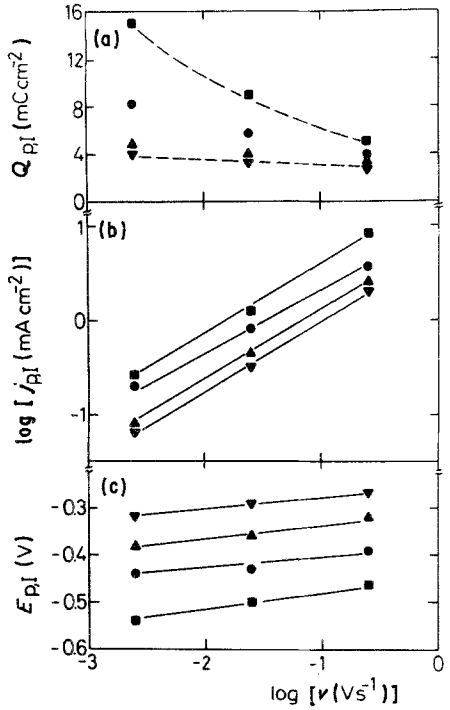

Fig. 6. Dependences of $Q_{p,I}$ (a), $j_{p,I}$ (b) and $E_{p,I}$ (c) on v from voltammograms run in 0.5 M K_2CO_3 at $w = 0$ at different temperatures. (▼) 0° C; (▲) 25° C; (●) 50° C; (■) 75° C.

increases with temperature (Fig. 6b), and at a constant temperature the $E_{p,I}$ against log v plots exhibit reasonable linear relationships with a slope equal to 0.036 ± 0.008 V (decade)$^{-1}$ (Fig. 6c). At constant v, the value of $E_{p,I}$ shifts more negatively on increasing the temperature with a temperature coefficient close to -3 mV K^{-1}. On the other hand, at low v the influence of w on peaks I and I′ at different temperatures is similar to that indicated in Fig. 2b.

The Arrhenius plots for $j_{p,I}$ when $w = 0$ and $v = 0.0025$ V s^{-1} (Fig. 7a), and for $j_{p,I'}$ when $w = 2620$ r.p.m. and $v = 0.025$ V s^{-1} (Fig. 7b), furnish apparent activation energy values (ΔE^*) for the electrochemical processes associated with Peaks I and I′ of $\Delta E^*_{p,I} = 20.1$ kJ mol^{-1} and $\Delta E^*_{p,I'} = 15.5$ kJ mol^{-1}, respectively.

3.3. *System Ni/Solution C*

For the sake of comparison, measurements were carried out in 0.5 M K_2CO_3 at 25° C, pH 11.7, with KCl additions up to 2 M in order to study the influence of KCl on the relative contributions of anodic peaks I and I′. Voltammograms (not shown) obtained in the entire v range with quiescent solutions shows that neither $Q_{p,I}$ nor $j_{p,I}$ are affected by the presence of KCl. Nevertheless, under stirring at constant KCl concentration, the value of $j_{p,I}$ diminishes, and that of $j_{p,I'}$ increases with increasing w (Fig. 8). This effect is clearly observed by comparing, for instance, voltammograms in Figs 2b and 8. Furthermore, it should be noted that the voltammograms associated with the $Ni(OH)_2$/NiOOH redox couple at high positive potentials are considerably influenced in shape and charge by the concentration of KCl (Fig. 9). However, in 0.5 M K_2CO_3 solution pitting was observed only for the concentration ratio $c_{Cl^-}/c_{OH^-} > 200$, whereas in the absence of carbonate ions intensity pitting of nickel in alkaline media was already detected for $c_{Cl^-}/c_{OH^-} > 1$, in agreement with data previously reported in the literature [18]. These results suggest that chloride ions accelerate the dissolution of the prepassive layer although carbonate ions contribute to increased stability of the passive layer.

3.4. *System Ni/Solution D*

The voltammetric behaviour of nickel in stagnant carbonate–bicarbonate solutions covering wide ranges of pH and ionic strength reveals that the parameters of Peak I at constant pH become practically independent

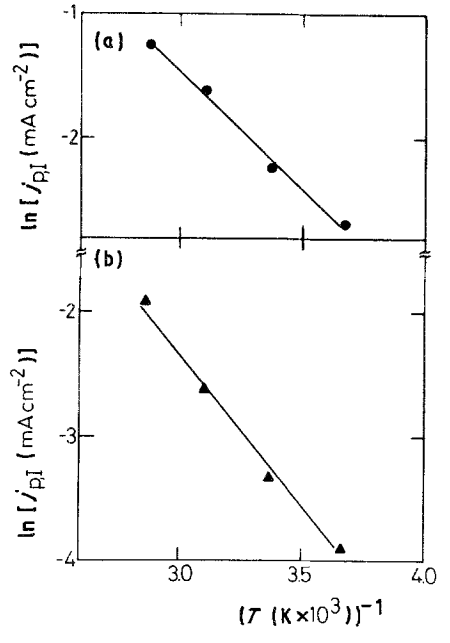

Fig. 7. Arrhenius plots corresponding to $j_{p,I}$ at (a) $w = 0$ and (b) $w = 2620$ from voltammograms run in 0.5 M K_2CO_3 at $v = 0.0025$ V s^{-1}.

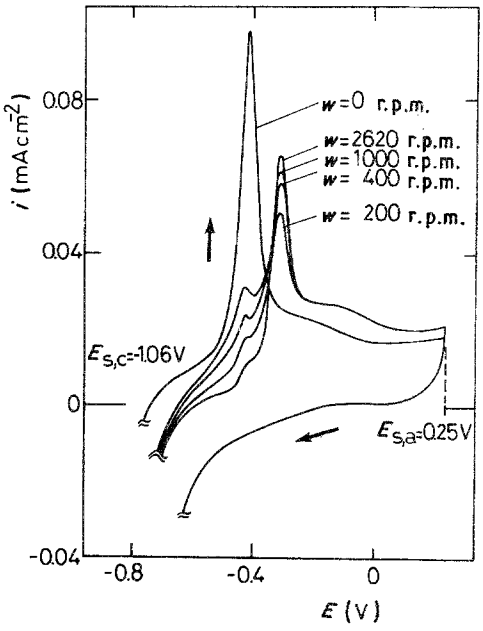

Fig. 8. Influence of w in the voltammograms run in 0.5 M K_2CO_3 + 2 M KCl at $v = 0.0025$ V s^{-1}.

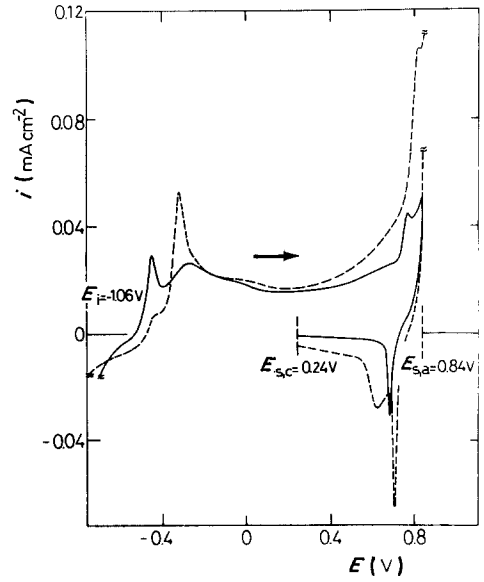

Fig. 9. Influence of KCl concentration added to 0.5 M K_2CO_3 on the voltammograms run at $v = 0.0025\ V\ s^{-1}$ and $w = 2620$ r.p.m. (——) 0.0001 M KCl; (----) 1 M KCl.

of the electrolyte concentration, and at a constant v, only slightly influenced by pH (Fig. 10). On the other hand, data obtained for Peak I′ at $w = 2620$ r.p.m. and $v = 0.0025\ V\ s^{-1}$ in the entire range of the solution composition show that the dependence of $j_{p,I'}$ on pH varies with the concentration of one anion fixed as an independent variable, keeping the concentration of the other anion constant (Fig. 11). Thus, at a constant bicarbonate ion concentration (full lines in Fig. 11) $j_{p,I'}$ is practically independent of pH, whereas at constant carbonate ion concentration (dashed lines in Fig. 11) linear log $j_{p,I'}$ against pH relationships can be drawn with slopes of -0.5 ± 0.1.

The potential transients resulting for anodic current steps (Fig. 12) show three clear transition times. The first corresponds to the voltammetric level of peak I, the second lies in the potential range of peak I′ and the third appears at potentials more positive than the potential where the Ni(III) oxidation level starts. The

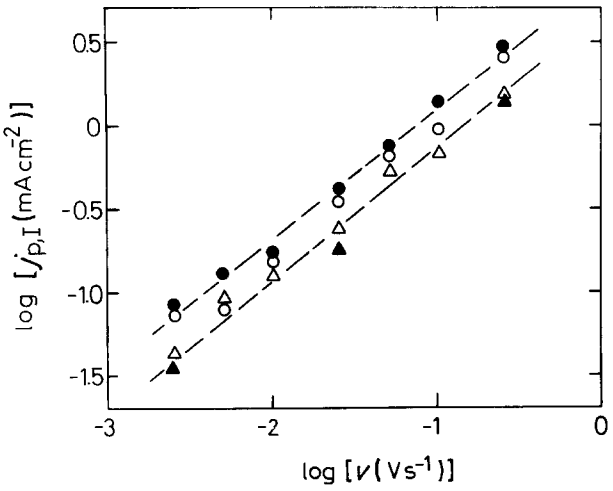

Fig. 10. Dependence of $j_{p,I}$ on v from voltammograms run at $w = 0$ in (○) 0.75 M $KHCO_3$ + 1.5 M K_2CO_3 and (●) 0.075 M $KHCO_3$ + 0.15 M K_2CO_3 at pH = 10.54 and in (△) 0.75 M $KHCO_3$ + 0.005 M K_2CO_3 and (▲) 0.075 M $KHCO_3$ + 0.0005 M K_2CO_3 at pH = 8.35.

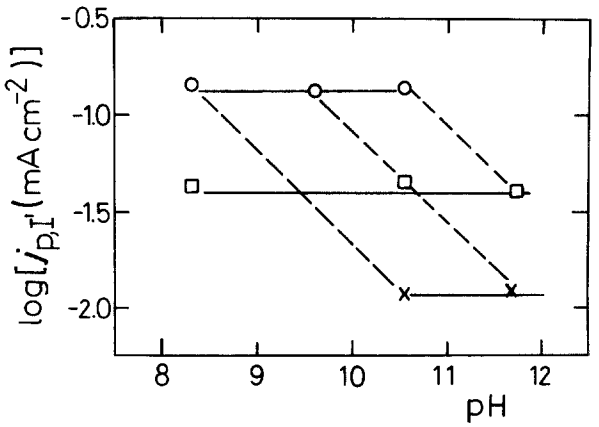

Fig. 11. Dependence of $j_{p,I'}$ on pH for different carbonate–bicarbonate solution composition from voltammograms run at $v = 0.0025\ V\ s^{-1}$ and $w = 2620$ r.p.m. Full lines correspond to solution compositions at constant $KHCO_3$ concentrations: (○) 0.75 M $KHCO_3$; (□) 0.075 M $KHCO_3$; (×) 0.0075 M $KHCO_3$. Dotted lines indicate the corresponding solution compositions at constant K_2CO_3 concentration.

third transition time is presumably related to the OER. A change of slope in the transient at about 0.5 V is also noticed, which is at present difficult to correlate with the corresponding voltammogram. On the other hand, the potential transients resulting for a cathodic current step depend on the initiation potential. A greater HER depolarization effect can be observed as the initiation potential is set more positively. Furthermore, when the initiation potential is in the OER region, two transition times can be recorded, the first is probably related to the electroreduction of higher nickel oxyhydroxide and the second presumably related to the O_2 electroreduction reaction. Otherwise, anodic current transients recorded from $E_{j=0}$, the potential at which the current is close to zero during a positive potential-going excursion at low v, up to different potentials (see potential against time plot inset in Fig. 13), E_τ, within the potential region of $Ni(OH)_2$ forma-

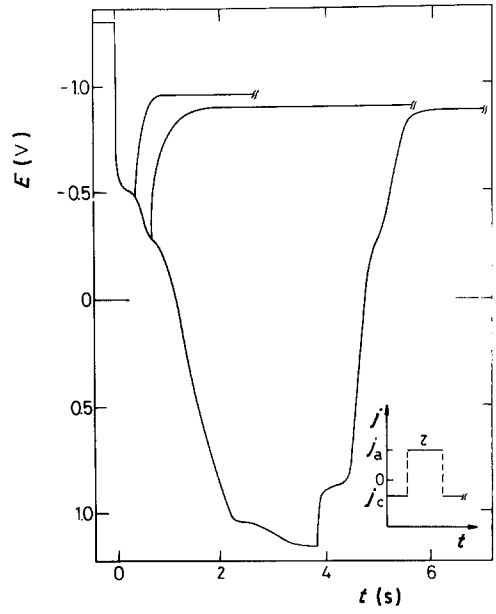

Fig. 12. Galvanostatic charging at $j_a = 0.08$ (mA cm^{-2}) and discharging at $j_c = -0.03$ (mA cm^{-2}) at w, curves in 0.15 M K_2CO_3 + 0.075 M $KHCO_3$.

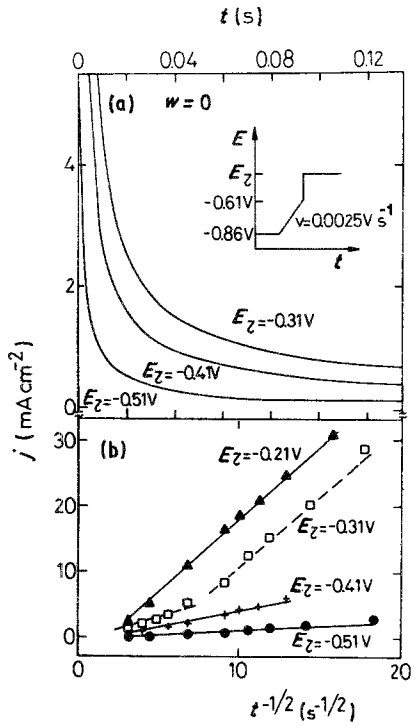

Fig. 13. (a) Anodic current transients recorded in 0.15 M K_2CO_3 + 0.075 M $KHCO_3$ during the potential holding at E_τ with the perturbation programme depicted in (b) j against $t^{-1/2}$ plots derived from data corresponding to the current transients at different E_τ.

tion, exhibit a continuous current decay which increases as the amount of anodic layer produced at E_τ increases (Fig. 13a). The corresponding j against $t^{-1/2}$ plots (Fig. 13b) present single linear relationships when E_τ is set in the potential range of Peak I, whereas for E_τ values fixed in the potential region of Peak I′ the slope of the straight lines attain a constant value at short times, but this decreases at large times when E_τ is set more negatively.

4. Discussion

The anodic behaviour of nickel in CO_3^{2-}/HCO_3^- buffers as followed through voltammetry (Figs 1 and 8), galvanostatic (Fig. 12) and potentiostatic (Fig. 13) current transients can be described in terms of reactions involving the Ni/Ni(II) oxidation level in the −0.8 V to 0 V range (Fig. 1), and the Ni(II)/Ni(III) oxidation level in the 0.4–0.9 V range (Fig. 9). At the first oxidation level, the formation of a thin hydrated $Ni(OH)_2$ [15] ($K_{sp} = 5.47 \times 10^{-16}$ at 25° C [2]) layer at $E < -0.3$ V takes place, followed by the appearance of a basic nickel carbonate salt layer at > -0.3 V, as expected from the solubility product of $NiCO_3$ ($pK_s = 8.18$ at 25° C) [21]. This means that the reactions occurring in the potential range of peaks I–I′ can be associated with the following stoichiometric equations:

$$Ni + H_2O \rightleftharpoons Ni(OH)_2 + 2H^+ + 2e^- \quad (1a)$$

$$Ni(OH)_2 + CO_3^{2-} \rightleftharpoons NiCO_3 + 2OH^- \quad (1b)$$

$$Ni(OH)_2 + HCO_3^- \rightleftharpoons Ni^{2+} + CO_3^{2-} + OH^- + H_2O \quad (1c)$$

$$Ni^{2+} + CO_3^{2-} \rightleftharpoons NiCO_3 \quad (1d)$$

The electrochemical parameters of the Ni/Ni(II) reaction appear to be considerably dependent upon the solution composition, namely the HCO_3^-/CO_3^{2-} concentration ratio and pH. Thus, for Peak I, in the absence of Cl^- ion in solution, one obtains:

$$\left(\frac{\partial \log j_{p,I}}{\partial \log v}\right)_{pH} \simeq 1;$$

$$\left(\frac{\partial E_{p,I}}{\partial \log v}\right)_{pH} \simeq 0.060\ \text{V (decade)}^{-1} \quad (2)$$

$$\left(\frac{\partial \log j_{p,I}}{\partial \log c_{CO_3^{2-}}}\right)_{pH,v} = \left(\frac{\partial \log j_{p,I}}{\partial \log c_{HCO_3^-}}\right)_{pH,v} \simeq 0 \quad (3)$$

$$\left(\frac{\partial \log j_{p,I}}{\partial\ pH}\right)_{c_{CO_3^{2-}},v} = \left(\frac{\partial \log j_{p,I}}{\partial\ pH}\right)_{c_{HCO_3^-},v} \simeq 0 \pm 0.1 \quad (4)$$

On the other hand, for Peak I′ at constant v:

$$\left(\frac{\partial \log j_{p,I'}}{\partial \log c_{CO_3^{2-}}}\right)_{pH} = \left(\frac{\partial \log j_{p,I'}}{\partial \log c_{HCO_3^-}}\right)_{pH} \approx 0.5 \quad (5)$$

$$\left(\frac{\partial \log j_{p,I'}}{\partial\ pH}\right)_{c_{CO_3^{2-}}} \approx -0.5 \quad (6)$$

$$\left(\frac{\partial \log j_{p,I'}}{\partial\ pH}\right)_{c_{HCO_3^-}} \simeq 0 \quad (7)$$

Equations 6 and 7 can be correlated by further considering the carbonate–bicarbonate ionic equilibrium:

$$HCO_3^- = CO_3^{2-} + H^+; \quad pK = 10.33 \text{ at } 25°\text{C} \quad (8)$$

$$z'_{HCO_3^-} = \left(\frac{\partial \log j_{p,I'}}{\partial \log c_{HCO_3^-}}\right)_{c_{CO_3^{2-}}} = \left(\frac{\partial \log j_{p,I'}}{\partial \log c_{H^+}}\right)_{c_{CO_3^{2-}}} \times \left(\frac{\partial \log c_{H^+}}{\partial \log c_{HCO_3^-}}\right)_{c_{CO_3^{2-}}} \simeq (0.5) \times (1) \simeq 0.5 \quad (9)$$

$$z'_{CO_3^{2-}} = \left(\frac{\partial \log j_{p,I'}}{\partial \log c_{CO_3^{2-}}}\right)_{c_{HCO_3^-}} = \left(\frac{\partial \log j_{p,I'}}{\partial \log c_{H^+}}\right)_{c_{HCO_3^-}} \times \left(\frac{\partial \log c_{H^+}}{\partial \log c_{CO_3^{2-}}}\right)_{c_{HCO_3^-}} \simeq (0) \times (-1) \simeq 0 \quad (10)$$

To obtain $z'_{HCO_3^-}$ and $z'_{CO_3^{2-}}$, the pseudo reaction orders involved at Peak I′ with respect to the HCO_3^- and CO_3^{2-} concentrations, respectively, account must also be taken of the fact that the voltammetric charge of Peak I′ depends on the electrolyte composition. Thus:

$$z'_{HCO_3^-} = \left(\frac{\partial \log j_{p,I'}}{\partial \log c_{HCO_3^-}}\right)_{c_{CO_3^{2-}}} = \left(\frac{\partial \log j_{p,I'}}{\partial \log Q_{p,I'}}\right)_{c_{CO_3^{2-}}} \times \left(\frac{\partial \log Q_{p,I'}}{\partial \log c_{HCO_3^-}}\right)_{c_{CO_3^{2-}}} \simeq (2.1) \times (0.23) \simeq 0.5 \quad (11)$$

$$z'_{CO_3^{2-}} = \left(\frac{\partial \log j_{p,I'}}{\partial \log c_{CO_3^{2-}}}\right)_{c_{HCO_3^-}} = \left(\frac{\partial \log j_{p,I'}}{\partial \log Q_{p,I'}}\right)_{c_{HCO_3^-}} \times \left(\frac{\partial \log Q_{p,I'}}{\partial \log c_{CO_3^{2-}}}\right)_{c_{HCO_3^-}} \simeq (0.1) \times (0) \simeq 0 \quad (12)$$

The passivation of Ni in carbonate–bicarbonate solutions at alkaline pH values can be discussed within the framework of the general reaction pathway recently postulated to interpret the potentiodynamic behaviour of nickel in still and stirred sulphuric acid–potassium sulphate solutions in the 0.4–5.7 pH range [22]. In alkaline solutions both $Ni(OH)_2$ and $NiCO_3$ can contribute to passive layer formation due to their low solubility products. Therefore, the probable anodic reaction comprises the fast formation of $Ni(OH)_{ad}$ which occurs in strong acid [23] and alkaline [24] solutions according to modulated cyclic voltammetry. The reaction takes place through an adsorbed intermediate which participates in a surface exchange process yielding an Ni [OHNi] surface species which can produce $Ni(OH)_2$ and/or soluble Ni(II) through parallel reactions [22]. The relative contribution of these two reactions depends on the local pH, which, in the present case is determined by v, w and the local buffer capacity of the CO_3^{-2}/HCO_3^- system, and on the OH^-/HCO_3^- at the metal surface concentration ratio. Otherwise, the chemical dissolution of the primary $Ni(OH)_2$ layer as soluble Ni(II) should be assisted by local low pH values, and, eventually, by the presence of aggressive anions. This offers another possibility of producing $Ni(OH)_2$ surface species through the precipitation of $Ni(OH)_2$ close to the electrode surface. The film which causes nickel to passivate in aqueous solutions was identified by *in situ* differential reflectometry in conjunction with XPS techniques as $Ni(OH)_2$ [25, 26].

On the assumption that low potential sweep rate voltammetry approaches the quasi-stationary state conditions, the anodic reaction can be interpreted as a complex reaction mechanism based, in the early stages, on $Ni(OH)_2$ formation [19, 20] and the possible ionic equilibria involved at the reaction interface. Thus, for $E < -0.3$ V, the Ni–OH^- interaction should be stronger than the Ni–HCO_3^- interaction and, therefore, the anodic reaction can be explained through reaction pathway I (below), where, as discussed earlier, Step 3 becomes rate determining. In the reaction scheme k denotes the number of surface sites available for the reaction. Anodization at this potential mainly favours the formation of $Ni(OH)_2$ (full trace) [27] and probably also, to a minor extent, $NiCO_3$ (dashed trace) under local buffering produced by the CO_3^{-2}/HCO_3^- system. This reaction pathway explains that, at large v, the reaction involves only the $Ni(OH)_2$ monolayer level and that any chemical reaction involving the dissolution of the anodic layer by the presence of HCO_3^- ions is, to a large extent, impeded.

As already discussed in previous publications [19, 20] reaction pathway I under Step 3 as rds, accounts for the experimental kinetic parameters already shown for Peak I. In this case $j_{p,I}$ becomes practically independent of pH because the degree of surface coverage by the absorbed intermediate is also independent of pH at any v. The experimental activation energy derived from the temperature dependence of Peak I is consistent with a place exchange reaction such as that represented by Step 3. This type of rate controlling reaction explains the mechanism of the anodic oxide layer formation at the level up to that of a few monolayers on several metals [28–32].

The anodic reaction for $E > -0.3$ V involves the appearance of Peak I′, which is influenced by w, pH and HCO_3^- ion concentration. When the applied potential exceeds -0.3 V, the composition of the interface changes considerably. Thus, a certain amount of H^+ ions have been produced, forcing the action of the buffer system. Under these circumstances, a possible reaction between OHNi species and HCO_3^- ions should be enhanced (Step 5), particularly under stirring. Another possibility, involves the direct interaction between HCO_3^- ions and $Ni(OH)_2$ (Steps 5′ and 6′). In both cases the final product of the anodic reaction is principally $NiCO_3$.

It should be noted that a complexing effect of HCO_3^- ions for transition metal oxides has been

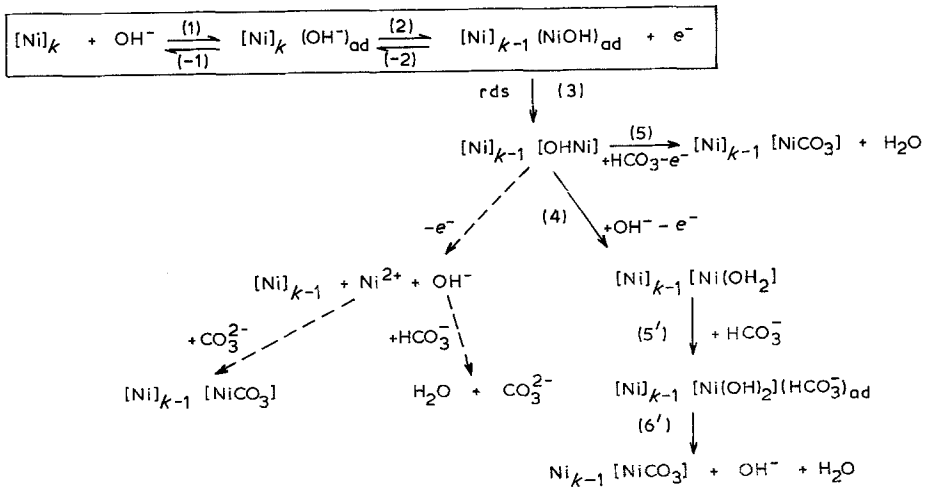

Pathway I

demonstrated for Co in alkaline solutions containing carbonate buffer [14] and for passive nickel oxide at high potentials [33]. For $w = 0$, the local buffer effect is limited so that one should expect $Ni(OH)_2$ as the main product in the potential range of Peak I, as occurs for other solutions. Conversely, stirring should have the opposite effect. The entire process is favoured by both stirring, which supplies HCO_3^- ions, and low v, as the latter increases the time for the chemical reaction. These facts are in qualitative agreement with the experimental findings. The charge involved in the formation of the anodic layer under stirring is about twice that obtained for still solution.

The formation of $NiCO_3$ through Steps 3 and 5 or Steps 3 to 6′ can explain the 0.5 reaction order with respect to HCO_3^- ion concentration. This fractional reaction order can be interpreted in terms of a Temkin adsorption behaviour for the reaction intermediates, in the same way as for the electrodissolution kinetics of nickel in acid solutions containing Cl^- ions [34, 35].

In the presence of a large concentration of Cl^- ions in the solution, the high specific adsorbability of Cl^- ions, which is well known for the iron family metals [3, 8, 36, 37] implies a competitive adsorption at the metal surface level between these ions and OH^- ions. On the basis of this assumption, the interpretation of the process under rotation, that is, when a rapid supply of aggressive ions to the reaction layer is assured, can be tentatively advanced through reaction pathway II.

Accordingly, the formation of the $NiCO_3$ multilayer proceeds through metal attack by the aggressive anion. Therefore, the overall effect of Cl^- ions in the CO_3^{2-}/HCO_3^- system is to enhance the formation of $NiCO_3$, that is, to increase the contribution of Peak I′, to a large extent at the expense of Peak I (Fig. 9). Nevertheless, at low v and $w = 0$, the local accumulation of OH^- species determines the prevalence of Peak I, as the preferred reaction pathway becomes presumably closely related to that depicted in reaction pathway I.

The preceding interpretation, based upon a bifurcation of the reaction pathway, is consistent with the potentiostatic current transient data for the oxide layer formation. Thus, the current transients which fit

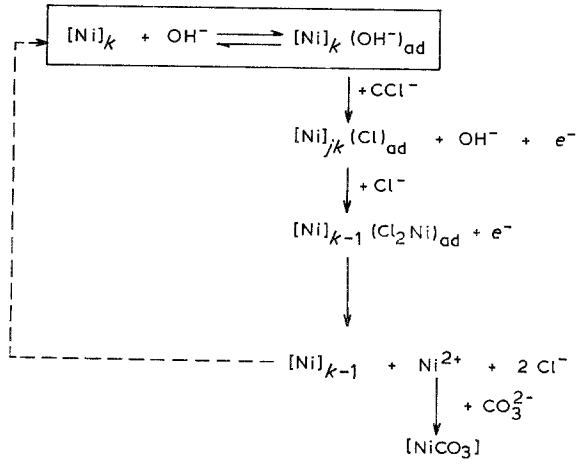

Pathway II

linear j against $t^{-1/2}$ relationships going through the origin, show two interesting features. Firstly, for $E > -0.3$ V and for $E < -0.4$ V there are single slopes as one should expect for an apparently single kinetic law obeyed through the entire process. Otherwise, at intermediate values of E, a break in the plots is observed, each portion obeying a linear relationship. These results are consistent with the formation of two distinct anodic layers in different potential ranges. The kinetic laws related to passive layer formation in the absence of Cl^- ions probably involve a nucleation and growth mechanism under diffusion control. It should be noted that the type of behaviour just described is qualitatively comparable to that already reported for the pitting corrosion of nickel in near neutral buffered solutions containing 0.1–1 M NaCl [38]. In addition, it also correlates with the time variation of the amount of electric charge passed in film formation on nickel at pH 8.42 and pH 11.5 at constant potential, $E =$ 0.645 V, in borate and phosphate solutions containing 0.5 M NaCl [39], which exhibits an inflexion between two stages of the process.

5. Conclusions

In CO_3^{2-}/HCO_3^- containing solutions the kinetics of $Ni(OH)_2$ formation, as followed through voltammetry, galvanostatic and potentiostatic current transients, is modified due to the presence of HCO_3^- ions. The charge involved in the passive layer corresponds to the thickness of a few monolayers and its composition involves both $Ni(OH)_2$ and $NiCO_3$ species. Competing reactions at the reaction intermediate level contribute to the formation of the composite passivating layer.

The formation of $Ni(OH)_2$ prevails at lower potentials and can be explained through a surface process with a rate determining step related to a place exchange reaction. Otherwise, the complexing effect of HCO_3^- ions on the oxygen containing surface species produced during anodization at higher potentials accounts for the formation of $NiCO_3$ at the passive layer level. The participation of HCO_3^- ions in the anodic process is assisted both by stirring and by the local change in pH related to the anodization reaction. Under comparable conditions, the influence of HCO_3^- ions also becomes evident in Cl^--containing solutions. The entire process can be interpreted through a complex reaction pathway which operates in alternative directions as the composition of the interface changes during the potential sweep in the positive potential-going direction.

References

[1] N. Maki and N. Tanaka, in 'Encyclopedia of Electrochemistry of the Elements', Vol. III (edited by A. J. Bard), Marcel Dekker, New York (1975) pp. 43–210.
[2] A. J. Arvia and D. Posadas, in *ibid.* pp. 212–421.
[3] R. P. Frankenthal and J. Kruger (eds), 'Passivity of Metals', The Electrochemical Society Inc., Princeton, New Jersey (1978).
[4] D. H. Davies and G. T. Burstein, *Corros. Sci.* **20** (1980) 973.
[5] *Idem, ibid.* **20** (1980) 989.
[6] *Idem, Corrosion* **36** (1980) 416.
[7] G. Nazri, E. Yeager and B. D. Cahan, Technical Report

No. 1, Proj. NR SR0-009/7-30-79, Case Western Reserve University, Cleveland (1981).
[8] K. E. Heusler, in 'Encyclopedia of Electrochemistry of the Elements', Vol. IX-A (edited by A. J. Bard) Marcel Dekker, New York (1982) pp. 229–381.
[9] L. M. Gassa, J. R. Vilche and A. J. Arvia, *J. Appl. Electrochem.* **13** (1983) 135.
[10] M. Fremont (ed.), 'Passivity of Metals and Semiconductors', Elsevier Amsterdam (1983).
[11] M. E. Vela, J. R. Vilche and A. J. Arvia, *J. Appl. Electrochem.* **16** (1986) 490.
[12] O. R. Valentini, C. A. Moina, J. P. Vilche and A. J. Arvia, *Corros. Sci.* **25** (1985) 985.
[13] E. B. Castro, C. R. Valentini, C. A. Moina, J. R. Vilche and A. J. Arvia, *ibid.* **26** (1986) 781.
[14] C. A. Gervasi, S. R. Biaggio, J. R. Vilche and A. J. Arvia, *ibid.* **29** (1989) 427.
[15] A. E. Bohé, J. R. Vilche and A. J. Arvia, *J. Appl. Electrochem.* **14** (1984) 645.
[16] M. S. Abdel Aal and A. H. Osman, *Corrosion* **36** (1980) 591.
[17] N. Jallcrat, F. L. Pari, F. Bourelier and K. Vu Quang, Proceedings of the 9th International Congress on Metal Corrosion, Toronto, Vol. 4 (1984) pp. 404–6.
[18] J. Postlethwaite, *Electrochim. Acta* **12** (1967) 333.
[19] R. S. Schrebler Guzmán, J. R. Vilche and A. J. Arvia, *Corros. Sci.* **18** (1978) 765.
[20] J. R. Vilche and A. J. Arvia, in 'The Nickel Electrode' (edited by R. G. Gunther and S. Gross), The Electrochemical Society Inc., Pennington (1982) pp. 19–47.
[21] L. Maites (ed.), 'Handbook of Analytical Chemistry', McGraw-Hill, New York (1963) pp. 1–17.
[22] M. R. Barbosa, S. G. Real, J. R. Vilche and A. J. Arvia, *J. Electrochem. Soc.* **135** (1988) 1077.
[23] S. G. Real, J. R. Vilche and A. J. Arvia, *Corros. Sci.* **20** (1980) 563.
[24] R. S. Schrebler Guzmán, J. R. Vilche and A. J. Arvia, *J. Appl. Electrochem.* **9** (1979) 321.
[25] R. E. Hummel, R. J. Smith and E. D. Verink Jr., *Corros. Sci.* **27** (1987) 803.
[26] *Idem, ibid.* **27** (1987) 815.
[27] J. R. Vilche and A. J. Arvia, in 'Passivity of Metals' (edited by R. P. Frankenthal and J. Kruger), The Electrochemical Society Corrosion Monograph Series, Princeton (1978) pp. 861–77.
[28] E. Lanyon and F. E. Trapnell, *Proc. R. Soc. London Ser.* A **227** (1955) 387.
[29] M. A. Genshaw, in 'Electrosorption' (edited by E. Gileadi), Plenum Press, New York (1967) p. 81.
[30] K. J. Vetter and J. W. Schultze, *Ber. Busenges. Phys. Chem.* **75** (1971) 4701.
[31] *Idem, J. Electroanal. Chem.* **34** (1972) 141.
[32] Z. Cataldi, R. O. Lezna, M. C. Giordano and A. J. Arvia, *J. Electroanal. Chem.* **261** (1988) 61–75.
[33] N. Sato, K. Kudo and M. Miki, *J. Jpn Inst. Metals* **35** (1971) 10.
[34] A. Bengali and K. Nobe, *J. Electrochem. Soc.* **126** (1979) 1118.
[35] S. G. Real, M. Barbosa, J. R. Vilche and A. J. Arvia, *J. Electrochem. Soc.* in press.
[36] J. R. Vilche and A. J. Arvia, *Anal. Acad. Cs. Ex. Fis. Nat. Buenos Aires* **33** (1981) 33.
[37] W. J. Lorenz and K. E. Heusler, In 'Corrosion Mechanism' (edited by F. Mansfeld), Marcel Dekker, New York (1987) p. 1.
[38] D. V. Vázquez Moll, R. C. Salvarezza, H. A. Videla and A. J. Arvia, *J. Electrochem. Soc.* **132** (1985) 754.
[39] R. Nishimura, *Corrosion* **43** (1987) 486.